

PAPER

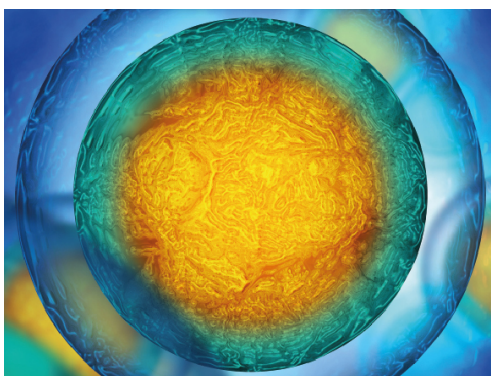
Avian whiffling-inspired gaps provide an alternative method for roll control

To cite this article: Piper Sigrest and Daniel J Inman 2022 *Bioinspir. Biomim.* **17** 046014

View the [article online](#) for updates and enhancements.

You may also like

- [Fault diagnosis and accommodation for multi-actuator faults of a fixed-wing unmanned aerial vehicle](#)
Zhenbao Liu, Lina Wang, Yuecheng Song et al.
- [Design and experimental verification of smart aileron structure based on Shape Memory Alloy](#)
S W Liu and F Li
- [Computational Investigations of Small Deploying Tabs and Flaps for Aerodynamic Load Control](#)
C P van Dam, R Chow, J R Zayas et al.



Biophysical Society | **IOP | ebooks™**

Your publishing choice in all areas of biophysics research.

Start exploring the collection—download the first chapter of every title for free.

Bioinspiration & Biomimetics



PAPER

Avian whiffing-inspired gaps provide an alternative method for roll control

RECEIVED
2 December 2021REVISED
1 May 2022ACCEPTED FOR PUBLICATION
24 May 2022PUBLISHED
15 June 2022Piper Sigrest*  and Daniel J Inman 

Department of Aerospace Engineering, University of Michigan, Ann Arbor, MI, United States of America

* Author to whom any correspondence should be addressed.

E-mail: psigrest@umich.edu**Keywords:** rapid descent, banking, spoiler, aileron, bio-inspiration, avian whiffing, roll controlSupplementary material for this article is available [online](#)

Abstract

Some bird species exhibit a flight behavior known as whiffing, in which the bird flies upside-down during landing, predator evasion, or courtship displays. Flying inverted causes the flight feathers to twist, creating gaps in the wing's trailing edge. It has been suggested that these gaps decrease lift at a potentially lower energy cost, enabling the bird to maneuver and rapidly descend. Thus, avian whiffing has parallels to an uncrewed aerial vehicle (UAV) using spoilers for rapid descent and ailerons for roll control. However, while whiffing has been previously described in the biological literature, it has yet to directly inspire aerodynamic design. In the current research, we investigated if gaps in a wing's trailing edge, similar to those caused by feather rotation during whiffing, could provide an effective mechanism for UAV control, particularly rapid descent and banking. To address this question, we performed a wind tunnel test of 3D printed wings with a varying amount of trailing edge gaps and compared the lift and rolling moment coefficients generated by the gapped wings to a traditional spoiler and aileron. Next, we used an analytical analysis to estimate the force and work required to actuate gaps, spoiler, and aileron. Our results showed that gapped wings did not reduce lift as much as a spoiler and required more work. However, we found that at high angles of attack, the gapped wings produced rolling moment coefficients equivalent to upwards aileron deflections of up to 32.7° while requiring substantially less actuation force and work. Thus, while the gapped wings did not provide a noticeable benefit over spoilers for rapid descent, a whiffing-inspired control surface could provide an effective alternative to ailerons for roll control. These findings suggest a novel control mechanism that may be advantageous for small fixed-wing UAVs, particularly energy-constrained aircraft.

1. Introduction

Certain bird species, especially waterfowl, sometimes turn their bodies upside down mid-flight while keeping their heads level, in a maneuver known as whiffing (figure 1) [1]. Whiffing is typically described as tumbling or side-slipping, and is cited as a method of rapid descent commonly seen in geese [2–6] during landing [2–4] or predator evasion [5, 7]. Larger birds such as the black stork (*Ciconia nigra*) have also been observed whiffing during courtship displays [8]. These previous studies are largely qualitative and observational, and recent studies focus on whiffing with respect to neck control and head stabilization,

rather than aerodynamic performance or control [1, 9].

Since whiffing is used for rapid descent, it is probable that it decreases lift, likely by allowing airflow through 'gaps' between twisted feathers. On the upstroke during normal flight, airflow from the dorsal to the ventral side of the wing twists the primary flight feathers open and creates gaps along the trailing edge of the wing [11–13]. When a bird flips over to whiffle, the airflow is again dorsal to ventral, and twists the primary feathers open. Airflow through the resulting gaps could decrease lift while the bird is in a whiffing position (figure 2). While primary feathers are known to twist in such flow [11–13], there are no quantified results of secondary feathers twisting while whiffing. Note that the term 'whiffing'



Figure 1. Whiffing greylag goose (*Anser anser*). Photograph taken on the Norfolk Broad England. Reproduced with permission from [10].

refers to the behavior of flying upside down, while feather twisting is a mechanism that occurs during the whiffing behavior and other situations characterized by dorsal-to-ventral airflow.

The rapid descent and extreme maneuverability associated with whiffing provides useful inspiration for improving the control of fixed-wing uncrewed aerial vehicles (UAVs). Just like birds whiffle, UAVs can use spoilers to decrease lift and increase drag, thus descending without building up excessive speed [15]. For the purposes of this work, we characterize rapid descent as a decrease in coefficient of lift and an increase in coefficient of drag. Although not known to be possible or used by birds, we speculated that hypothetically whiffing only one wing would create a net rolling moment due to the decreased lift from the whiffled wing, thus causing roll like an aileron. These similarities between avian whiffing and conventional fixed-wing control surfaces led us to hypothesize that a whiffing-inspired control surface could provide a beneficial alternative method of rapid descent and roll control for fixed-wing energy-constrained UAVs. Therefore, in this work, we investigated two maneuvers (and their associated control surfaces) with parallels to whiffing: rapid descent controlled by a spoiler, and banking controlled by an aileron.

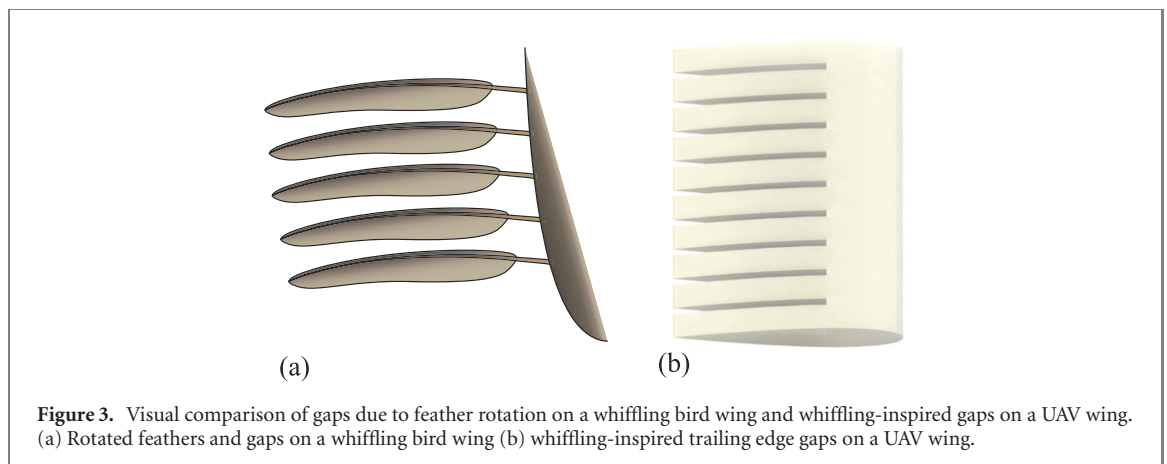
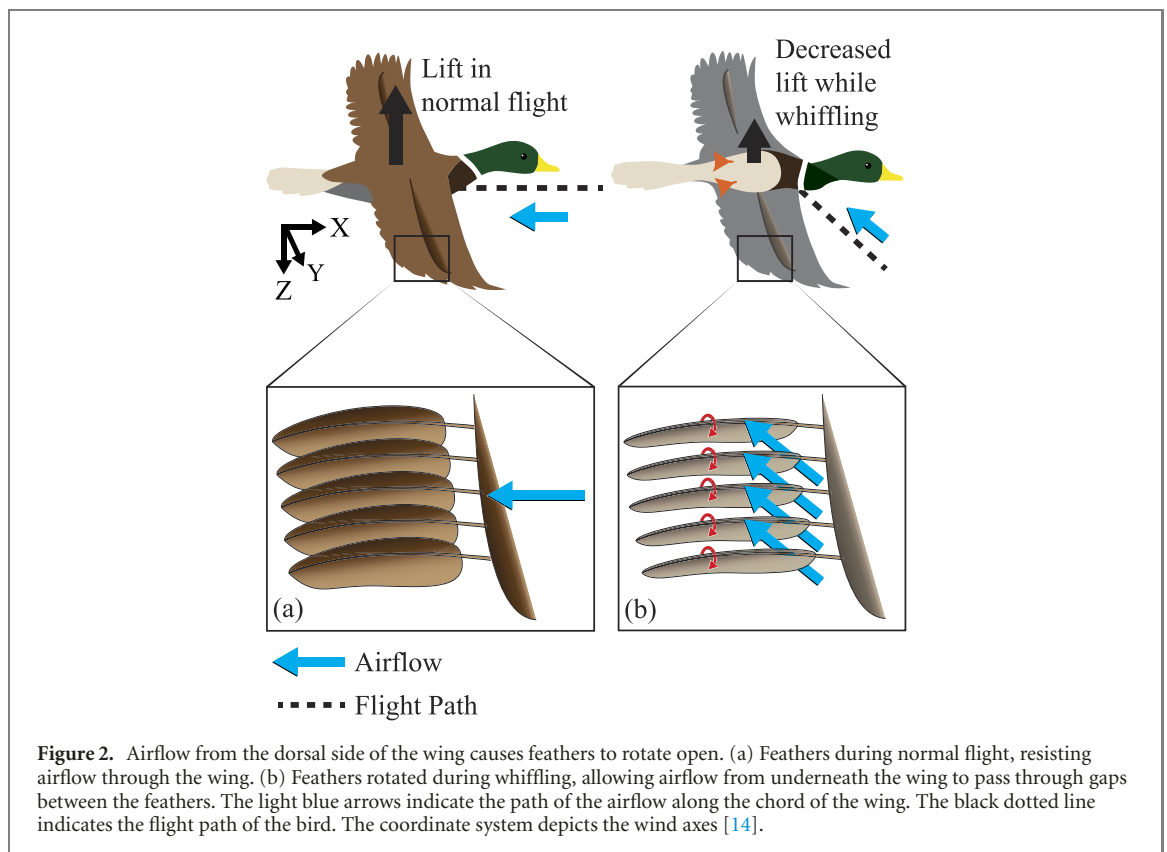
Combining the feather rotation mechanism of whiffing with practical energy considerations, we designed whiffing-inspired rectangular wings with a series of gaps in the trailing edge (figure 3). This wing design was particularly tailored to small UAVs, which are often challenged with limited payload volumes, power supplies with low energy densities, or constraints imposed by operating logistics or mission profiles. These obstacles make it important to reduce the energy cost of normal flight maneuvers, like descent and banking. While conventional spoilers and ailerons deflect into the flow, the gapped wing would operate in the same plane as the wing. Thus, the whiffing-inspired control surface could potentially

lower the actuation requirements, and therefore the energy cost, of rapid descent and banking maneuvers.

Birds typically have cambered wings [16], which would become inversely cambered during whiffing and could further contribute to decreasing lift. Inverted-camber wings have also been previously studied in numerous contexts, including inverted leading edge flaps, inverted wings in ground effect, and morphing trailing edges [17–19]. To focus our study solely on the effects of wing gaps, we did not investigate the effects of camber on whiffing, and instead based our design on in-plane gap actuation. However, the extent to which the camber and gaps—caused by feather rotation—interact to affect whiffing is unclear and requires future research.

The proposed gapped wings are similar to other technologies such as serrated trailing edges, split flaps, slotted spoilers, and slotted airfoils. Serrated trailing edges have been studied mainly for noise reduction [20], but few aerodynamic analyses have been conducted. Note that serrated trailing edges are physically unique from the wing gaps investigated in the current study [20]. Split flaps perforated with circular holes [21, 22] and slots [21] have been studied as dive brakes, but their purposes were to limit dive speed, reduce buffeting, and increase aileron control effectiveness during dives, rather than inducing descent or rolling [21, 22]. Furthermore, dive brakes on powered aircraft were intentionally designed to have minimal impact on lift production, which is unfavorable for rapid descent [21]. Slotted spoilers have also been investigated, but as a method of increasing aileron control effectiveness during a dive, rather than a method of descent [23]. Finally, slotted airfoils have been used to increase lift and delay flow separation at high angles of attack, however, such slots are typically cut along the span of the wing, perpendicular to orientation of the gaps in this study [24–27].

Here, we investigated if gaps in the trailing edge of a wing provided desirable control capabilities,



possibly similar to rotated feathers during whiffing, without requiring a UAV to fly inverted. We evaluated our hypothesis by characterizing the lift, drag, rolling moment, and yawing moment coefficients of trailing edge gaps using static wind tunnel tests on 3D printed wings. Next, we compared our aerodynamic results to previously published data on a representative spoiler for rapid descent, and a representative aileron for banking. This comparison included calculating equivalent deflection angles for the conventional control surfaces. Finally, we used kinematics to estimate the force and work required to operate a hypothetical gapped wing control surface, and compared these actuation requirements to previously published data on spoiler and aileron actuation. This research ultimately informs the development of a

control surface for energy-constrained UAV banking or rapid descent.

Finally, it is important to note that this study is founded on the principle of bioinspiration, rather than biomimicry. Our goal was not to replicate avian whiffing, rather, we observed the behavior and used it as the motivation for a novel control mechanism.

2. Materials and methods

2.1. Experimental setup for gapped wings

Wings with zero, three, five and nine gaps ($n = [0, 3, 5, 9]$) spaced evenly along the trailing edge ('gapped wings') were tested in a wind tunnel. We 3D printed the wings with ABS plastic on a Dimension Elite printer. Each wing had a rectangular planform

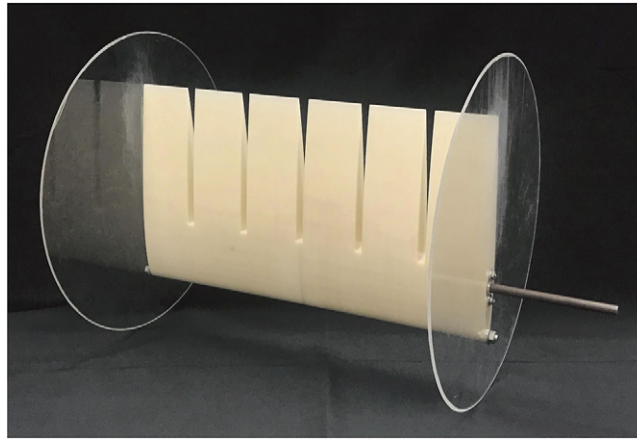


Figure 4. Fully assembled five-gap wing with end plates and mounting rod.

with a 16 in half span ($b = 16$ in.) and a 9 in. chord ($c = 9$ in.), yielding an aspect ratio of 3.56. A NACA 0012 airfoil was used for each wing, because of its symmetry and the wide availability of previously published aerodynamic data. The size of the gaps was held constant, with a gap length equal to $2/3$ the chord ($c_g = 6$ in.) and width equal to $1/48$ of the half span ($b_g = 1/3$ in.). For the nine-gap wing, this gap size yielded an area 12.5% less than the area of the wing with no gaps. We used the wing with no gaps as a ‘baseline wing’ to provide a reference point for the gapped wings.

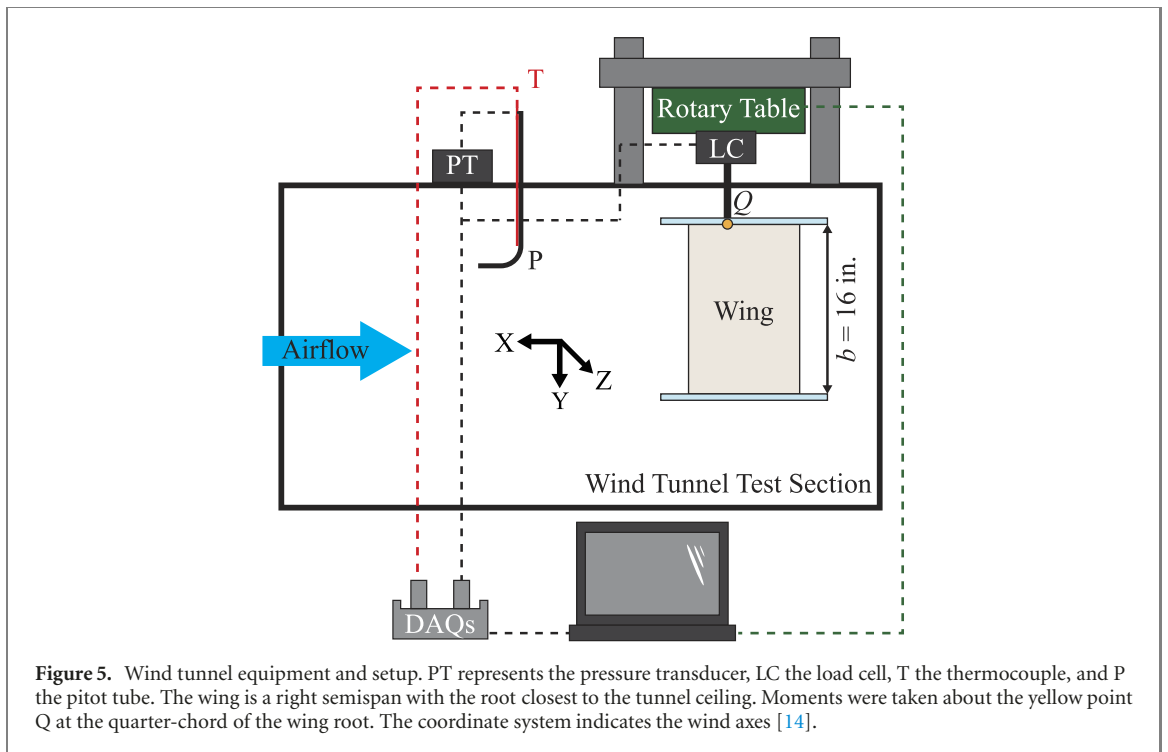
We installed circular end plates on either side of each wing to simulate two-dimensional flow, to study the effects of the gaps independently from the effects of wingtip vortices (figure 4) [28]. Due to the use of end plates, the data did not capture three-dimensional wing (tip) effects. Tip effects tend to reduce the coefficient of lift and the lift curve slope, and increase drag (through the creation of induced drag) [29]. It has also been found that, for a wing with a retractable aileron (morphologically similar to a spoiler deployed on the upper surface of one wing), increasing aspect ratio tends to increase rolling moment coefficient [30]. Since two-dimensional wings (with no tip effects) can be approximated as wings with an aspect ratio approaching infinity, this trend implies that tip effects tended to decrease rolling moment. The same study found as aspect ratio increased, the yawing moment became more favorable (in the same direction as roll) at low angles of attack, but more adverse (in the opposite direction as roll) at higher angles [30]. However, since adverse yaw is a result of tip effects, we refrain from describing the gapped wing yawing moment coefficients as ‘adverse’ or ‘proverse’. The two-dimensional effects of the endplates could be verified in the future through surface visualization techniques.

The wing assembly was mounted to a six-axis load cell (ATI delta force/torque sensor) with a rod at the quarter-chord. The load cell was affixed to a

rotary table (Parker Rotary Positioner 30012-S powered by a Vexta Stepper Motor PK266-03B), which was installed inverted on top of the test section. The wings were considered as half span right wings, with the root closest to the tunnel ceiling.

We conducted testing in a 2 ft \times 2 ft open-loop wind tunnel with a freestream turbulence level of 0.7% along the centerline, and approximately 1.8% near the edges of the tunnel [31]. The wings were mounted vertically from the test section ceiling with 3.25 in. of clearance between the end plate and the ceiling of the tunnel, to ensure the wing was sufficiently outside the wall boundary layer. We measured temperature data with a type T thermocouple, and dynamic pressure with a pitot tube and Omega PX-2650 pressure transducer. Load cell data were collected at each angle of attack for 5 s at a rate of 3600 Hz. We automated the tests and data collection using MATLAB scripts. Figure 5 shows the test setup.

We performed three trials of each wing at a Reynolds number (Re) of 2.33×10^5 , corresponding to a velocity (V) of 16.1 m s^{-1} . The Re was within a range comparable to birds and UAVs [32]. Before each trial, we ran a tare sweep from -20° to 0° in 1° increments, with the wind tunnel off. We found the tare to be consistent across angles based on its low standard deviation across angle of attack. Therefore, for ease of calculations, we used the tare values at 0° angle of attack in subsequent data analysis. The zero-degree angle of attack was found by sweeping through a small range of near-zero angles, then interpolating to find the angle at which the normal force on the wing vanished. Following from the airfoil’s symmetry, we set this zero-lift angle of attack to be 0° angle of attack. During each trial, we swept the wing from 0° to 10° (1° increments) and from 10° to 20° (0.5° increments), which provided sufficient resolution in the stalled regions. The effective angle of attack range experienced by the wings varied slightly from this commanded range due to data corrections.



We found that hysteresis effects within a single trial were negligible.

2.2. Analysis of gapped wings experimental data

We averaged the results of the three trials at each angle of attack to present cumulative data, because each wing's individual trials were highly repeatable. The data were corrected for solid blockage, wake blockage, and jet boundaries following Barlow *et al* [14]. These corrections approximated freestream conditions and allowed for more direct comparison with other previously published data. No other corrections were made because they were deemed negligible. Given the thinness of the endplates, they were not included in the wing planform area when calculating the aerodynamic force and moment coefficients. We calculated the experimental uncertainty of the data according to the guide to the expression of uncertainty in measurements (GUM) and reported the expanded uncertainty of the data with a level of confidence of approximately 95% [33]. To quantify if the differences between each gapped wing and the baseline wing were statistically significant, we calculated the expanded uncertainty of the difference of means at an approximately 95% confidence level. Appendices A and B further detail the uncertainty and statistical analyses.

To avoid conflating the aerodynamic effects of the end plates with the effects of varying the number of gaps, we reported the aerodynamic parameters as incremental values, that is, the difference between the gapped wing and the baseline wing values. The results are therefore intended to be taken in a comparative context between wings with different numbers of gaps. For rapid descent, we also considered the gapped wings to be symmetrical (having the same

number of gaps on the left and right semispans), since spoilers are deployed symmetrically. For example, the incremental coefficient of lift ΔC_L was calculated as the difference between the coefficient of lift of the baseline wing and the gapped wing:

$$\Delta C_L = \frac{L_g}{qS_g} - \frac{L_b}{qS_b}. \quad (1)$$

Where L is the measured lift force of the semispan wing (N), q is the dynamic pressure (Pa), S is the area of the semispan wing (m^2), the subscript g denotes the gapped wings, and the subscript b denotes the baseline wing. Note that the coefficients of lift of the gapped wings were normalized by the gapped wing planform area (the planform area of the baseline wing minus the planform area of all of the gaps). By doing so, we interpreted changes in coefficient of lift as results of the gaps themselves, rather than the decreased wing area. We calculated the incremental coefficient of drag in the same manner.

For the moments, we adopted the sign convention in which the positive moment directions are consistent with the positive conventions on the wind axes, shown in figures 2 and 5 [14]. Thus, a positive rolling moment is a roll towards the right wing [34]. To create a rolling moment, a UAV would need to use an asymmetric wing configuration, be it with ailerons or different gapped wings on each side. Pairing a right gapped semispan with a left baseline semispan would initiate a positive roll towards the right gapped wing due to the difference in lift production. Thus, a right gapped wing was comparable to an upwards deflected aileron on the right semispan. We presented the experimental moment results as a full wing with

a right semispan gapped wing and a left semispan baseline wing.

Moment coefficients were calculated about the point on the inner surface of the end plate at the wing root, at the quarter-chord (yellow point Q, figure 5). We calculated the moment coefficients of the full asymmetric wing by subtracting the moment coefficients of the baseline wing from those of the gapped wings [14]. The measured moments were normalized by the full wing area and span [14]. For example, the rolling moment coefficient C_l was calculated according to:

$$C_l = \frac{l_g}{qS_f(2 \cdot b)} - \frac{l_b}{qS_f(2 \cdot b)} \quad (2)$$

$$S_f = S_g + S_b = (bc) + (bc - nb_g c_g). \quad (3)$$

Where l_g is the measured rolling moment of the semispan gapped wing (N m), l_b is the measured rolling moment of the semispan baseline wing (N m), S_f is the full wing area, and b is the half span. We calculated the net yawing moment and the yawing moment coefficient in the same manner. Note that it is more desirable for the rolling moment to result in a yaw with the same sign, that is, in the same direction as the roll.

2.3. Gapped wing actuation estimates

To calculate the force and work required to actuate the gaps, we considered a hypothetical actuation scheme in which the gaps were nominally blocked by covers (the unactuated configuration). To actuate, the covers slid spanwise into recesses in the wing, leaving the gaps exposed (the actuated configuration). The recesses were thin walled, so the unactuated wing represented the baseline wing as closely as possible. The mock-up is shown in figure 6 with the gap covers in light blue.

We estimated the force required to actuate the gap covers based on kinematics:

$$F_g = n \cdot F_{fr} = n \cdot \mu F_N. \quad (4)$$

Where F_g is the force required to actuate all the gap covers (N), F_{fr} is the friction force acting on one gap cover (N), μ is the coefficient of static friction, F_N is the normal force acting on one gap cover (N), and n is the number of gaps. The lift force acting on the covers was estimated in the normal force term:

$$F_N = m_{gc}g - L_b \frac{(b_g \cdot c_g)}{bc}. \quad (5)$$

Where m_{gc} is the mass of a single gap cover (kg) and L_b is the measured lift force (N) of the baseline wing scaled to the area of the gap. To make comparisons between the gapped wings and conventional control surfaces as direct as possible, we used the baseline wing lift measured at the angle of attack corresponding to the equivalent control surface deflection. The

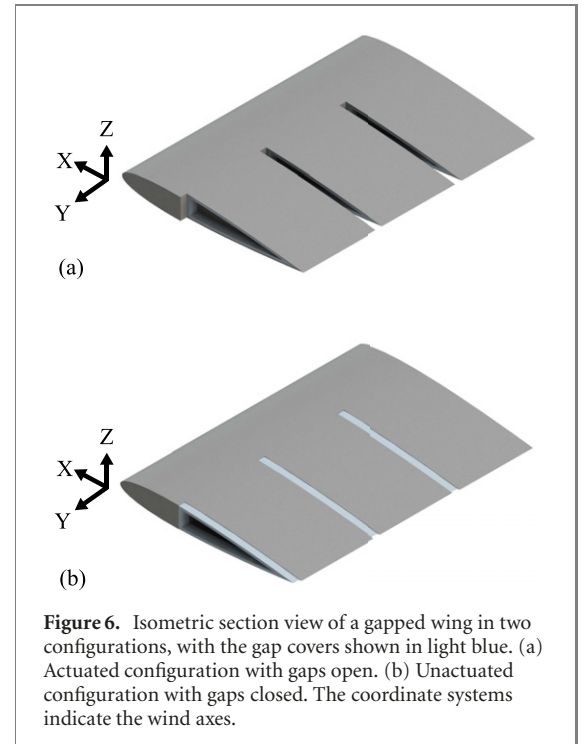


Figure 6. Isometric section view of a gapped wing in two configurations, with the gap covers shown in light blue. (a) Actuated configuration with gaps open. (b) Unactuated configuration with gaps closed. The coordinate systems indicate the wind axes.

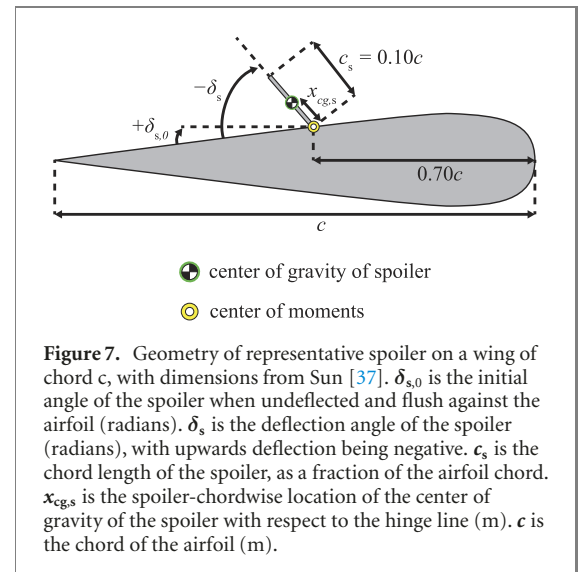


Figure 7. Geometry of representative spoiler on a wing of chord c , with dimensions from Sun [37]. $\delta_{s,0}$ is the initial angle of the spoiler when undeflected and flush against the airfoil (radians). δ_s is the deflection angle of the spoiler (radians), with upwards deflection being negative. c_s is the chord length of the spoiler, as a fraction of the airfoil chord. $x_{cg,s}$ is the spoiler-chordwise location of the center of gravity of the spoiler with respect to the hinge line (m). c is the chord of the airfoil (m).

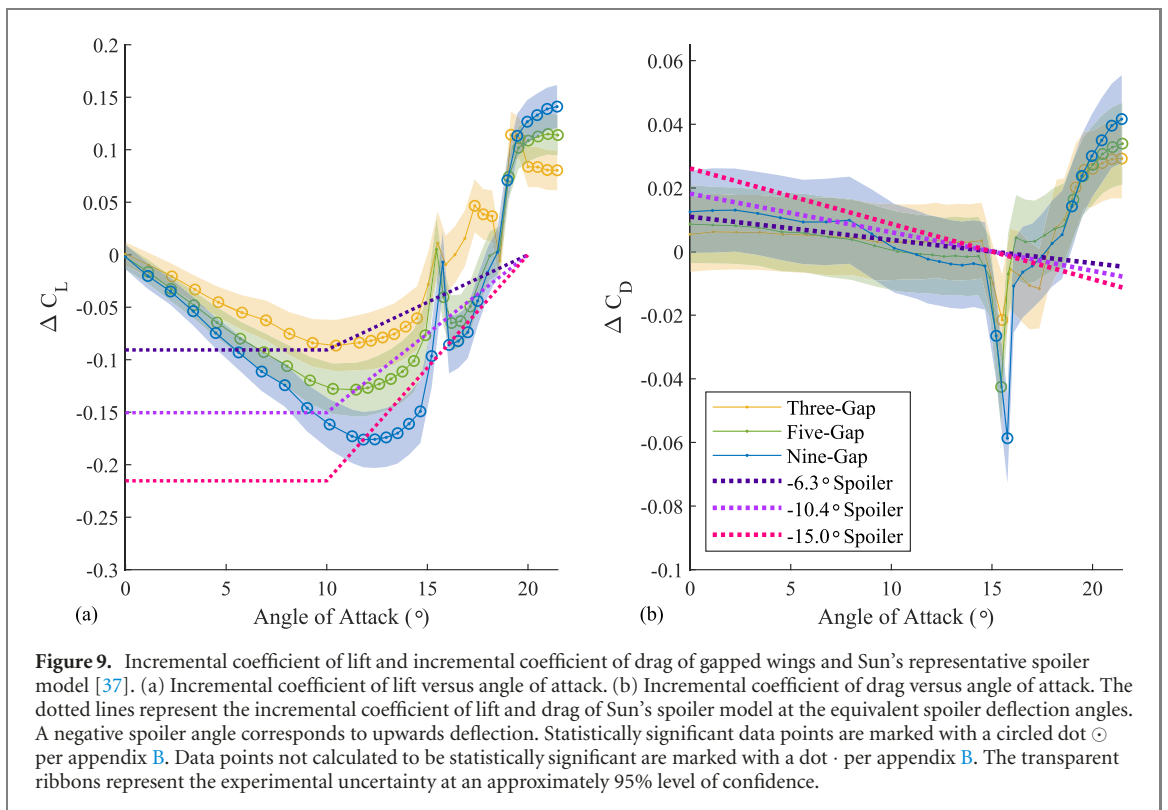
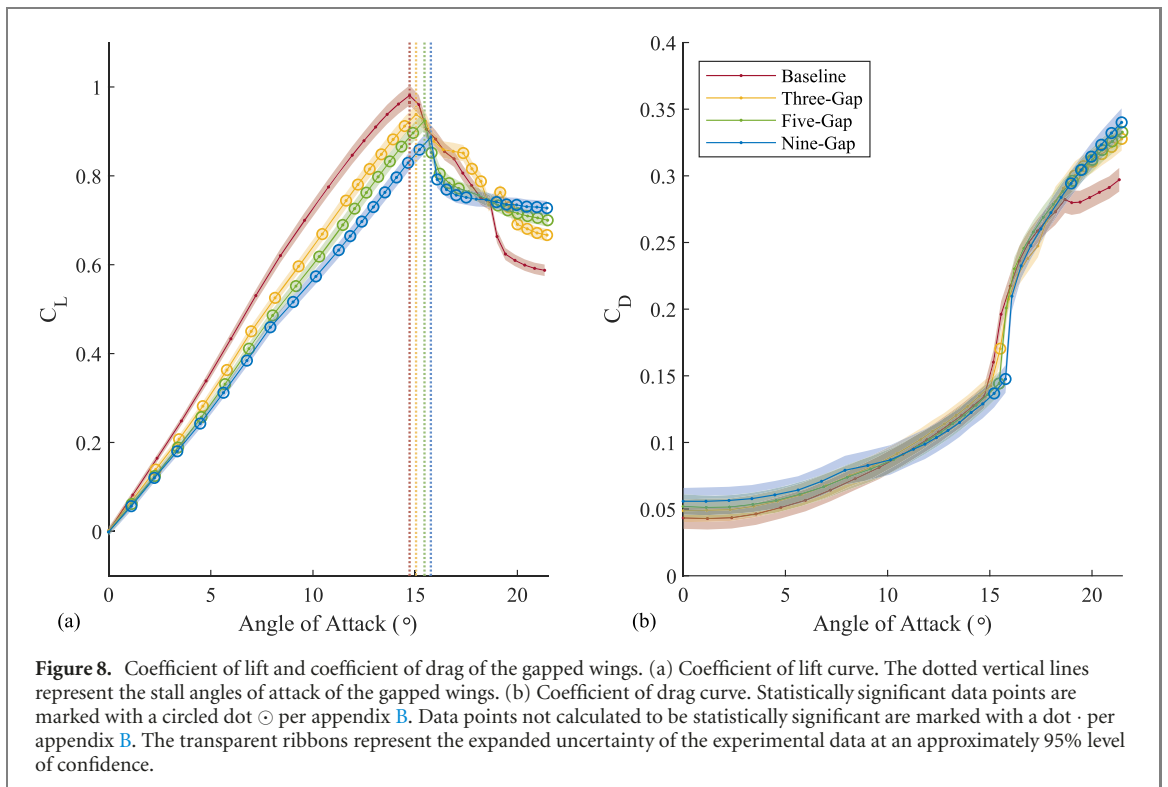
work required to actuate all of the gaps (J) was given by:

$$W_g = F_g \cdot b_g. \quad (6)$$

Where b_g is the gap width (m). For the gapped wings, we used a static coefficient of friction of 0.28 and a density of 1.01 g cm^{-3} , which are typical values for a generic ABS plastic [35, 36]. The volume of a single gap cover as modelled in CAD was 10.35 cm^3 .

2.4. Representative spoiler

For the rapid descent comparison, we considered a model of a representative spoiler developed by Sun [37]. Spoilers reduce lift to cause descent, and increase drag to prevent excessive buildup of speed. Sun's model described a full-span spoiler with a chord that was 10% of the wing chord, positioned at 70% chord,



with a maximum deflection of 60° (figure 7). The model was built with data from various spoilers with chords ranging from 5% to 15% wing chord, locations from 65% to 73% wing chord, on a variety of airfoils, at an Re from 2.8×10^5 to 71×10^6 [37]. The spoilers were mostly three-dimensional, with the exception of several two-dimensional studies [37].

Since our gapped wing experimental data extended up to 20° angle of attack, we used Sun's model that accounted for large angles of attack, where the incremental coefficient of lift (ΔC_L) and incremental coefficient of drag (ΔC_D) were given by:

$$\Delta C_L = 0.32\gamma_L\delta_s + 0.51\gamma_L \sin(\delta_s) \quad (7)$$

$$\Delta C_D = -0.1\gamma_D\delta_s \quad (8)$$

$$\gamma_L(\alpha) = \begin{cases} 1.0, & -10^\circ \leq \alpha < 10^\circ \\ 2.0 - \frac{\alpha}{10.0}, & 10^\circ \leq \alpha < 20^\circ \end{cases} \quad (9)$$

$$\gamma_D(\alpha) = 1.0 - \frac{\alpha}{15}, \quad -15^\circ \leq \alpha \leq 20^\circ. \quad (10)$$

Where α is the angle of attack (degrees) and δ_s is the deflection of the spoiler (radians). Sun defined the incidence influence functions γ_L and γ_D to generalize the lift and drag spoiler models (respectively) to larger angles of attack. As shown in figure 7, upwards spoiler deflections were negative, yielding negative coefficient of lift increments and positive coefficient of drag increments.

To compare the spoiler model to the gapped wing data, we calculated equivalent spoiler deflection angles for the representative spoiler on a wing with the same geometry and flow conditions as the baseline wing. We first determined the greatest reduction of coefficient of lift of each gapped wing, and the angle of attack at which it occurred. Since the focus of the rapid descent comparison was on lift reduction, this point represented the best-case performance of each gapped wing. Then, using Sun's model, we calculated the spoiler deflection that created an equivalent coefficient of lift reduction at the same angle of attack.

After comparing the aerodynamics of the spoiler and gapped wings, we considered actuation requirements. Spoiler actuation requirements are typically specified as hinge moments [34, 38]. However, since the gapped wings operated in plane and thus do not have hinge moments, we converted the spoiler hinge moments to be in terms of force and work. We calculated the hinge moment of the spoiler M_s at the equivalent deflection for each gapped wing by [39]:

$$M_s = \frac{1}{2}\rho V_l^2 \left(\frac{1}{2}C_{D,s} \sin^2(\delta_s) \right) S_s c_s + m_s g \cdot x_{cg,s} \cos(|-\delta_s| - \delta_{s,0} - \alpha). \quad (11)$$

Where ρ is the air density (kg m^{-3}), V_l is the air velocity at the spoiler location (m s^{-1}), $C_{D,s}$ is the coefficient of drag of the deflected spoiler, S_s is the area of the spoiler (m^2), m_s is the mass of the spoiler (kg), α is the angle of attack (in radians) and g is the acceleration due to gravity (m s^{-2}). The first term of equation (11) approximated the hinge moment due to aerodynamic forces, as proposed by Scholz [39]. We used Scholz's suggested values for $C_{D,s}$ of 1.8 and V_l of $1.14 \times V$ [39]. The second term was the hinge moment due to the weight of the spoiler, assuming a flat plate and geometry as shown in figure 7. From our CAD model of the representative spoiler on a wing with the same geometry as the baseline wing, the volume was 7.37 cm^3 , $x_{cg,s}$ was 0.011 m, and $\delta_{s,0}$ was 0.105 radians.

We used a density of 1.01 g cm^{-3} for a generic ABS plastic [35]. We estimated the work according to [38]:

$$W_s = M_s |\delta_s|. \quad (12)$$

The method for calculating the spoiler actuation force (F_s) required us to make several assumptions about the mechanics of the spoiler actuation system. Chakraborty proposed [38]:

$$F_s = \frac{G_k M_s}{\eta}. \quad (13)$$

Where G_k is the gearing ratio of the control surface actuation system (rad m^{-1}) and η is the efficiency of the actuation system. The gearing ratio G_k described the change in control surface deflection $\Delta\delta$ per linear extension Δx of the actuator [38]:

$$G_k = \frac{\Delta\delta}{\Delta x}. \quad (14)$$

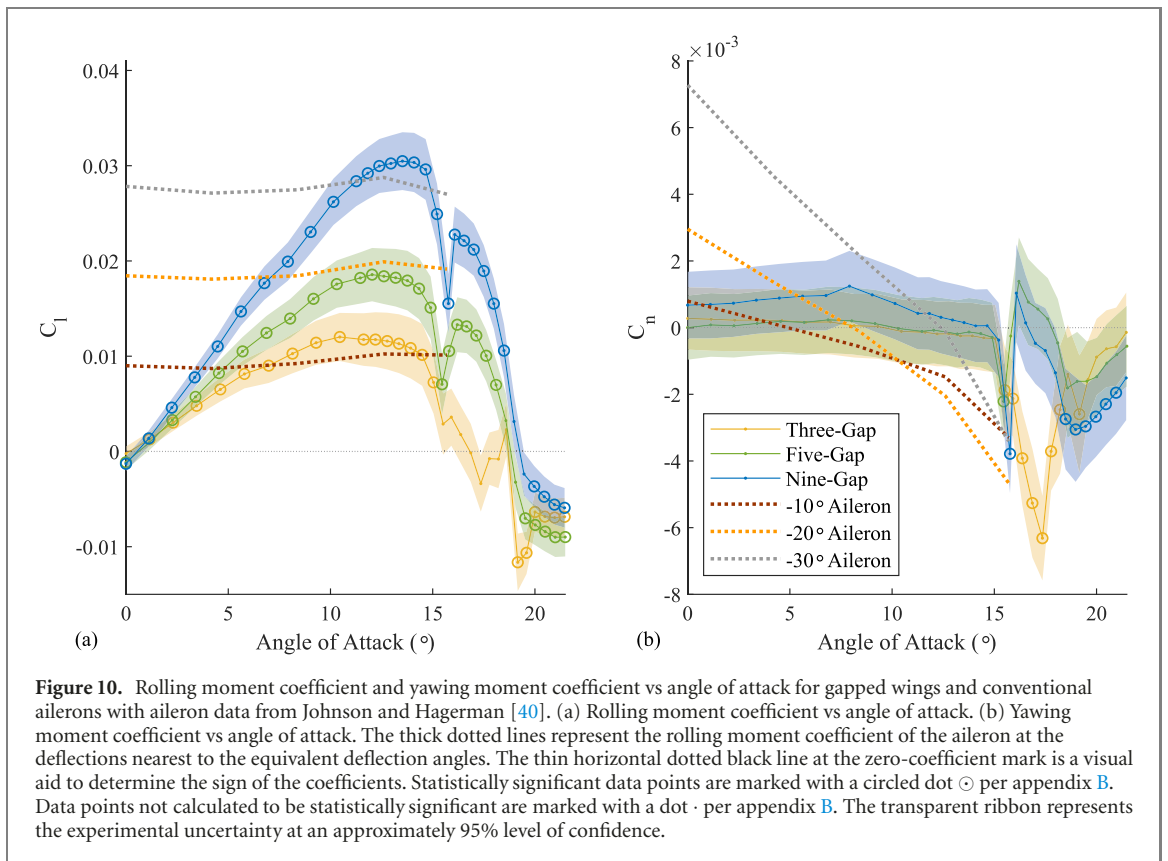
We stipulated that the spoiler was actuated by a servo motor with a control horn of radius 0.015 m. We assumed a one-to-one ratio between servo deflection and control surface deflection: a 60° servo rotation yielded a linear extension of 0.013 m, a spoiler deflection of 60° , and a gearing ratio of 80.6 m^{-1} . To make the comparison between gapped wings and spoiler conservative, and because no efficiency factor was applied to the hypothetical gapped wing control surface, we used an efficiency of 100%.

2.5. Representative aileron

For roll control, we compared the gapped wings to a three-dimensional wing with a representative aileron [40]. The aileron had a chord of 25% of the full wing chord and a span of 24.2% of the full span, positioned at the outboard tip of the right semispan [40]. These dimensions fell within the range of common aileron sizes [34], and there was published data on this aileron configuration from Johnson and Hagerman [40]. Most ailerons typically have a maximum deflection less than 25° to 30° [34, 40], as deflections past 20° to 25° could lead to flow separation and loss of control authority [34].

While Johnson and Hagerman used a symmetric NACA 64A010 airfoil [40], the NACA 64A010 and NACA 0012 two-dimensional coefficient of lift curves were nearly identical below stall [41], and had comparable stall angles on wings with similar aspect ratios [40]. The NACA 64A010 had a higher two-dimensional coefficient of drag [41], but the primary conclusions of this paper are based on coefficient of lift and rolling moment coefficient. Therefore, the difference in airfoils did not preclude comparison of the gapped wings with Johnson and Hagerman's aileron data.

According to the moments' sign convention, an upwards right aileron deflection was negative, and yielded a positive rolling moment towards the right



wing [34]. Thus, we compared the moments of a wing with a right gapped semispan and a left baseline semispan to a wing with a single upwards-deflected aileron on the right semispan.

We compared the representative aileron to each gapped wing using equivalent aileron deflection angles, for the representative aileron on a wing with the same geometry and flow conditions as the baseline wing. Since a higher rolling moment coefficient indicated better roll control, we first determined the maximum rolling moment coefficient of each gapped wing, and its corresponding angle of attack. Then, we linearly interpolated Johnson and Hagerman's data to find the aileron deflection that produced an equivalent rolling moment coefficient at the same angle of attack [40]. These equivalent aileron deflection angles were likely conservative: Johnson and Hagerman tested at a higher Re of 4.5×10^6 , meaning the ailerons likely produced larger coefficients of lift and rolling moment coefficients than they would at the Re of 2.33×10^5 used here [42]. At this lower Re , the aileron may create lower coefficients of lift and rolling moment coefficients, resulting in even higher equivalent aileron deflection angles.

Similarly to the spoiler, we calculated the aileron force and work from its hinge moments. We first interpolated Johnson and Hagerman's hinge moment coefficient data for the equivalent aileron deflections of each gapped wing. Johnson and Hagerman normalized the hinge moment by the first moment of area

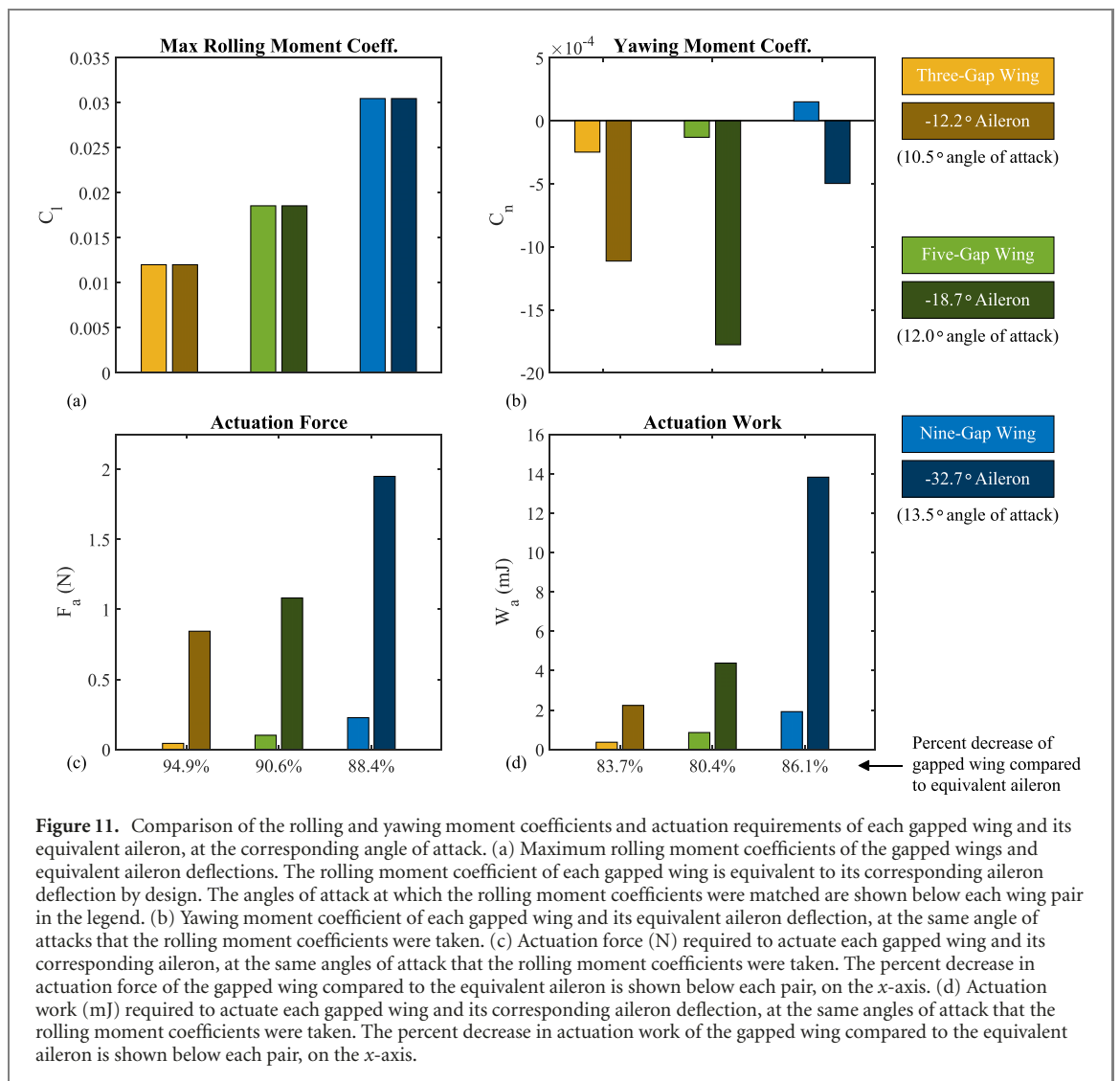
of the aileron [40], which was mathematically and numerically equivalent to normalizing by the product of the aileron area and aileron chord, as done here [34, 40]. We calculated the hinge moments M_a of each by:

$$M_a = \frac{1}{2} \rho V^2 C_h S_a c_a + m_a g \cdot x_{cg,a} \cos(|\delta_a| - \alpha). \quad (15)$$

Where V is the freestream velocity ($m s^{-1}$), S_a is the surface area of the aileron, m_a is the mass of the aileron (kg), and $x_{cg,a}$ is the chordwise location of the center of gravity of the aileron with respect to the hinge line (m). The first term of equation (15) was the moment due to aerodynamic loading, and the second term was the moment due to gravity acting on the aileron. We used the density of ABS plastic, an aileron volume of $41.06 cm^3$, and an $x_{cg,a}$ of $0.0196 m$ (from our CAD model of the representative aileron on a wing with the same geometry as the baseline wing). We then estimated the force and work required to deflect the aileron using the same method as the spoiler (equations (12)–(14)) assuming a gearing ratio of $80.6 m^{-1}$ and efficiency of 100%.

3. Results and discussion

The objective of the current research was to assess the gapped wings as alternatives to spoilers (for rapid descent) and ailerons (for banking) for energy-constrained UAVs. In the following subsections, we



first present the aerodynamic results of the gapped wings, then discuss effective control surface deflection angles and compare the aerodynamic results to spoilers and ailerons. Finally, we compare the actuation requirements of the gapped wings to the spoiler and aileron.

3.1. Aerodynamic results of gapped wings

We found that increasing the number of gaps significantly decreased the coefficient of lift below stall and lowered the maximum coefficient of lift of the wing (figure 8), even when normalized by the smaller gapped wing area. As the number of gaps increased, the wings stalled at a higher angle of attack. For example, the stall angle of attack increased by about 1° between the baseline and the nine-gap wing. The gapped wings also exhibited a sharper stall, indicated by more pointed peaks. Notably, the gapped wings experienced a smaller overall loss of lift due to stall than the baseline wing. A comparison of the baseline wing coefficient of lift with previously published NACA 0012 data can be found in the supplemental materials

(<https://stacks.iop.org/BB/17/046014/mmedia>) document.

We found that trailing edge gaps generally had an insignificant impact on the coefficient of drag. Minimal drag is typically considered advantageous for straight and level flight, climbs, and maneuvers, because lower drag requires less thrust and thus less energy to achieve the same airspeed. However, in the case of rapid descent, a larger drag coefficient can be beneficial in preventing excessive buildup of speed. At high angles of attack in the post-stall regime, the gapped wings did increase drag significantly compared to the baseline wing. But, the increase did not seem dependent on the number of gaps. For example, the nine-gap wing did not appear to produce significantly more drag than the three-gap wing.

The lift and drag phenomena exhibited by the gapped wing could be explained by airflow through the gaps from the pressure side of the wing to the suction side. This type of venting has been seen on slotted wings to reenergize the flow over the trailing edge and delay separation [24]. Wings with various slot configurations generally exhibit similar

Table 1. Actuation requirements of the nine-gap wing and -15.0° equivalent spoiler deflection, at 11.8° angle of attack. This scenario represented the best rapid descent performance of the gapped wings.

	-15.0° spoiler	Nine-gap wing
Hinge moment	0.0033 N m	N/A
Actuation force	0.267 N	0.182 N
Actuation work	0.865 mJ	1.54 mJ

lift behaviors to the gapped wings: decreased (or unaffected) lift at low angles of attack and increased lift at higher angles, relative to a baseline wing [24–27]. Some slotted wings also delayed stall [27], and others experienced a sharper stall [25], like the gapped wings. Furthermore, slotted airfoils generally increase drag, although the effects are usually small [24–27], much like the coefficient of drag of the gapped wings. While the performance similarities between the gapped wings and slotted wings may suggest they share similar flow mechanisms, further work is required to confirm this hypothesis for the gapped wings.

The lift and drag performance of the gapped wings in the post-stall region (specifically, above approximately 18.5°), has interesting implications for existing UAV rapid descent maneuvers that are performed at high angles of attack, like deep-stall [43]. To perform a deep-stall maneuver, a UAV increases angle of attack past stall, leading to flow separation and rapid lift reduction, in order to make a controlled descent [43]. At high angles of attack, increasing the number of gaps in the wing reduced the decay of lift, leading to a higher lift coefficient than the baseline wing. Initially, it would therefore seem the gapped wings may be less attractive for deep-stall. However, the gapped wings could provide a method to regulate descent during deep-stall, without requiring full stall recovery. For example, momentarily opening the gaps could recover a small amount of lift production, enabling a temporary lessening of the rate of descent. Further, the increased drag of the gapped wings at these high angles could enable a UAV to reduce its airspeed compared to the baseline wing. This effect would be particularly useful just prior to touchdown, if using a deep-stall maneuver to land, similar to birds [44]. Deep-stall is characterized by an extremely steep and fast descent [43], which requires stronger (and thus heavier) airframe to prevent damage upon touchdown. Opening gapped wings just prior to touchdown could soften the landing and reduce the need for heavier structures.

3.2. Comparison of spoiler and gapped wings for rapid descent

Figure 9 plots the incremental coefficient of lift and incremental coefficient of drag of the gapped wings compared to Sun's spoiler model at the equivalent deflection angles [37]. Figure 9 presents the same

Table 2. Equivalent aileron deflection angle and associated angle of attack of gapped wings.

Gapped wing	Equivalent deflection angle	At angle of attack
Three-gap	-12.2°	10.5°
Five-gap	-18.7°	12.0°
Nine-gap	-32.7°	13.5°

gapped wing data as figure 8, but in incremental format for comparison with the spoiler.

The greatest lift reduction of the gapped wings occurred with the nine-gap wing at 11.8° angle of attack, for which we calculated an equivalent spoiler deflection of -15.0° . In the most optimistic case, the gapped wings only captured the range of performance of a spoiler deflected -15° . However, recall that the maximum spoiler deflection angle is -60° . At lower angles of attack more commonly used for cruising and maneuvering flight, the gapped wings were even less effective at decreasing the coefficient of lift: at about 5° angle of attack the nine-gap wing decreased the lift coefficient only as much as a -6.3° deflected spoiler.

As dictated by Sun's model, the spoiler incremental coefficient of lift was constant for low angles of attack, then linearly increased above 10° angle of attack [37]. Conversely, the incremental coefficient of lift of the gapped wings was highly dependent on angle of attack. The lift reduction of both the gapped wings and the representative spoiler degraded at angles of attack above approximately 10° to 12° , making both control methods less effective for rapid descent at higher angles. However, while the spoiler could produce its greatest lift reduction across a range of angles of attack, the gapped wing could only achieve optimal performance at a narrow range of higher angles of attack.

The incremental coefficients of drag of the gapped wings were nearly constant below approximately 8° angle of attack. From 8° to 14° , the incremental coefficient of drag decreased gradually as the number of gaps increased. In the vicinity of stall, the incremental coefficient of drag of the gapped wings sharply became negative, before becoming positive again at high angles of attack. Except for high angles of attack, the gapped wings produced a small and insignificant incremental coefficient of drag. This effect was not necessarily desirable for rapid descent, because an increase in drag would help manage airspeed. Conversely, the spoiler coefficient of drag was positive below stall and generally produced greater drag than the corresponding gapped wings. The spoiler coefficient of drag gradually decreased as angle of attack increased.

To summarize the aerodynamic comparison between the gapped wings and representative spoiler, we found the gapped wings produced a less favorable response for rapid descent. The spoiler model was characterized by a significant decrease in lift and increase in drag, thus meeting our definition for

rapid descent. However, the gapped wings resulted in modest lift reduction and insignificant drag increase, so they did not meet all our requirements for rapid descent. Furthermore, the lift reduction of the gapped wings was highly dependent on angle of attack, while the spoiler lift reduction was constant below stall. Thus, the gapped wings appeared less aerodynamically desirable for rapid descent.

While the gapped wings did not perform as well as the representative spoiler, it was possible that the gapped wings could require less actuation force or work due to their planar operation, thus providing an advantage over the traditional spoiler. We calculated the force and work of the best-case scenario of the gapped wings (the nine-gap wing at 11.8° angle of attack), which corresponds to the spoiler model at the equivalent deflection angle -15.0° (table 1). Note that by design, the spoiler achieves rapid descent in this equivalent deflection case. The nine-gap wing required 31.7% less force but 78.3% more work than the equivalent spoiler.

In all, our aerodynamic and actuation results showed that the gapped wings did not provide a significant advantage for rapid descent over conventional spoilers. The gapped wings captured the coefficient of lift reduction of small spoiler deflections (up to -15.0°) and required higher actuation work.

3.3. Comparison of aileron and gapped wings for roll control

We found that increasing the number of gaps significantly increased the rolling moment coefficient (figure 10). The five-gap wing had an equivalent aileron deflection of -18.7° (at 12.0° angle of attack). This meant that the five-gap wing captured comparable performance to nearly the full range of the representative aileron, since maximum aileron deflections are typically 20° to 30° [34, 40]. Further, the nine-gap wing had an equivalent deflection angle of -32.7° (at 13.5° angle of attack) and was thus capable of producing rolling moment coefficients in excess of the maximum deflected aileron. Johnson and Hagerman only tested up to $\pm 30^\circ$ of aileron deflection, so we linearly extrapolated their data to determine the equivalent deflection angle of -32.7° for the nine-gap wing [40]. The equivalent deflection angles are summarized in table 2, and figure 11 shows the rolling moment coefficient and angle of attack used to determine each gapped wing's equivalent deflection. Note that the equivalent aileron deflections were calculated at angles of attack below stall of the respective gapped wing. Figure 10 displays the closest aileron deflections to the equivalent angles, rather than interpolations and extrapolations of Johnson and Hagerman's data [40].

Roll control effectiveness of an aileron can be estimated as the change in rolling moment coefficient per change in deflection angle [34]. However,

since the gapped wings do not deflect, the equivalent aileron deflection angle served as a measure of their roll control effectiveness. For example, at 13.5° angle of attack, a -32.7° aileron produced a rolling moment coefficient of 0.0305, yielding an estimated roll control effectiveness of 0.0534 per radian (given no rolling moment at the neutral aileron position [40]). The nine-gap wing produced the same rolling moment coefficient at this angle of attack, giving it an equivalent roll control effectiveness of 0.0534 per radian. Therefore, 'opening' nine gaps in the trailing edge had the same roll control effectiveness as deflecting an aileron 32.7° upwards, at that angle of attack. Since the rolling moment coefficient of the aileron remained fairly constant over angle of attack (figure 10), its roll control effectiveness also stayed relatively constant. Conversely, the rolling moment coefficient of the gapped wings varied strongly across angle of attack (figure 10): as angle of attack changed, so did the equivalent aileron deflection, and relatedly the roll control effectiveness. Thus, while the roll control effectiveness of the -32.7° aileron only dropped slightly as angle of attack went to zero, the roll control effectiveness of the nine-gap wing approached zero. In contrast, as angle of attack increased towards stall, the roll control effectiveness of the nine-gap wing exceeded that of the representative aileron, since the rolling moment coefficient of the nine-gap wing was greater than that of a maximum-deflected aileron.

Unlike the traditional aileron, which had relatively constant rolling moment coefficients over angle of attack, the coefficients of the gapped wings were highly dependent on lift. di Luca *et al* found similar trends with a bio-inspired morphing wing that folded its wing tips to change wing area [45]. Like di Luca's findings, we observed the gapped wings to be most effective at high coefficients of lift, meaning low-speed flight. According to di Luca, this low-speed regime is ideal for high maneuverability for small drones [45], and in these conditions, gapped wing roll control was superior to aileron control. However, the gapped wings did not create as large rolling moment coefficients as conventional ailerons at lower coefficients of lift. di Luca proposed a simple control workaround for the gapped wings' dependence on angle of attack: pairing the gapped wing actuation with a quick pitch-up movement would instantaneously increase coefficient of lift to achieve the maximum rolling moment coefficient [45]. The gapped wings could also be augmented with another control surface, such as a slotted flap or aileron, to provide higher rolling moment coefficients at lower coefficients of lift.

On a related note, gapped wings may also be more advantageous than ailerons at higher angles of attack because they increased stall angle of attack, and exhibited larger rolling moment coefficients at high angles of attack than the maximum deflected aileron. Aileron deflection angles above 20° to 25° tend to decrease stall angle of attack [34, 40]. Thus, if

a UAV flying at a high angle creates a rolling moment with a large aileron deflection, it is at risk of stalling. Conversely, the gapped wings delayed stall angle of attack. So, if a UAV flying at a high angle creates a rolling moment by opening gaps, it is at a lower risk of triggering stall. In addition, as seen in figure 10, the gapped wings created a much higher rolling moment coefficient than the maximum deflected aileron (30°) at high angles of attack.

These effects are especially poignant during flight at high angles of attack and low airspeed, such as short-field takeoff and slow-flight. Consider a UAV in slow-flight, flying in the vicinity of stall, that needs to perform a banking maneuver with ailerons. It can only make small aileron deflections or it risks stalling, and thus has a limited attainable rolling moment coefficient. If the UAV makes too large aileron deflections to achieve a higher rolling moment coefficient, it could stall prematurely. However, a UAV in slow flight with gapped wings would be able to create a much larger rolling moment coefficient with a lower risk of stall, because the gapped wings increase the stall angle of attack, and offer higher rolling moment coefficients than the maximum deflected aileron. Thus, the gapped wings may enable UAVs to roll at higher angles of attack and expand the maneuvering envelope.

At high angles of attack above about 18° , the rolling moment coefficient of the gapped wings became negative. This counterintuitively indicated a roll away from the gapped wing, and was due to the fact that the gapped wings produced a higher coefficient of lift than the baseline wing at these high angles (figure 8). This switch in rolling moment coefficient sign and the dependence of the rolling moment coefficient on angle of attack may also require a more complex controller that is capable of handling nonlinear aircraft models [46].

Note that the gapped wing rolling moment coefficients were slightly negative at 0° angle of attack. Since the gaps preserved the symmetry of the airfoil, and thus produced the same zero-lift as the baseline wing at 0° , we expected the rolling moment coefficient to be zero here. However, all the wings, including the baseline wing, produced a small (less than 0.01) but measurable rolling moment coefficient (before taking the difference with the baseline wing). Therefore, we attributed the non-zero rolling moment coefficient at 0° not to the gaps, but to experimental sources of variance that we were not reasonably able to quantify for the uncertainty analysis. These sources potentially included small manufacturing defects or asymmetries in the wings [14], slight compliance in the mounting scheme, or the type B variance of the load cell (discussed in appendix A).

The significant increase in rolling moment coefficient of the gapped wings was accompanied by a negligible rise in coefficient of drag (figure 8). While the insignificant change in coefficient of drag was not necessarily desirable for rapid descent, it is more

advantageous for roll control since a larger drag would require more thrust to maintain airspeed and altitude while banking. Higher drag differentials could also be tied to larger yawing moments.

In general, the yawing moment coefficient was not significantly impacted by the gaps, with the exception of some higher angles of attack. The yawing moment coefficient was relatively constant below stall, unlike the aileron, which steadily decreased as angle of attack increased. At low angles of attack, the gapped wings' yawing moment coefficient was the same sign as the rolling moment coefficient (positive). The three-gap and five-gap wing yawing moment coefficients became the opposite sign from roll around 10° , and the nine-gap wing around 15° . At higher angles of attack, the yawing moment coefficient of the three-gap wing remained the same sign as roll, while the sign of the five- and nine-gap wing switched again before ultimately returning to the same sign as the rolling moment coefficient. The roll-yaw coupling, and the fact that it changed sign multiple times, may require a more complex controller [47]. The coupling trend was also distinct from that of the ailerons: tip effects caused the aileron yawing moment coefficient to become steadily more negative as angle of attack increased, and the rolling moment coefficient stayed positive [40].

Figure 11 summarizes the rolling and yawing moment coefficients of the gapped wings and equivalent aileron deflections and illustrates several key trends. Firstly, as intended, the rolling moment coefficient of each gapped wing was equal to its equivalent aileron and increased as the gaps increased. Secondly, the gapped wing yawing moment coefficients grew steadily less negative as the number of gaps increased, such that the nine-gap wing yawing moment coefficient was positive (the same sign as the rolling moment coefficient). However, the yawing moment coefficients of the equivalent aileron deflections were all negative, and the opposite sign of the rolling moment coefficients.

While the gapped wings produced rolling moment coefficients equivalent to, and occasionally higher than, traditional ailerons, it was also important to compare actuation requirements. We found the gapped wings decreased actuation force by at least 88.4% and decreased actuation work by at least 80.4% compared to the equivalent aileron deflections (figure 11). The results of the aileron comparison indicated that the gapped wings may be a useful alternative to ailerons for roll control (figure 11). The gapped wings fully captured the range of rolling moment coefficients produced by a representative aileron. While there was not a clear benefit in yawing moment coefficients, the gapped wings required a fraction of the actuation work and force of the ailerons. The comparable roll control and lowered actuation costs make the gapped wings a potentially

beneficial alternative to traditional ailerons for banking control of energy-constrained UAVs, particularly at lower flight speeds.

4. Limitations and future work

The current research focused on the aerodynamic effects of trailing edge gaps on a symmetric airfoil. We neglected the potential role of bird wings' camber in our whiffing-inspired design. It is possible that replicating this work with a cambered wing would better approximate whiffing and produce greater changes in the coefficient of lift, rolling moment coefficient, and other parameters.

Since the spoiler model and representative aileron were three-dimensional wings, and the gapped wings approximated two-dimensional flow, it is important to consider the potential impact of tip effects on the comparisons. It was shown that the gapped wings do not decrease lift comparably to a spoiler. The lack of tip effects may have artificially increased the lift of the gapped wings [29], meaning this conclusion was conservative and three-dimensional gapped wings may have performed even less desirably than a spoiler. Conversely, because tip effects tend to increase drag [29], three-dimensional gapped wings may have a higher drag coefficient closer to that of the spoiler. In terms of roll control, decreasing aspect ratio tends to decrease the rolling moment coefficient [30]. This tip effect makes the comparison of the two-dimensional gapped wings to the representative aileron less conservative, since the three-dimensional gapped wing rolling moment coefficient may be lower than we measured. Decreasing aspect ratio makes the yawing moment more favorable at high angles of attack [30], but since the gapped wings were two-dimensional and thus could not produce adverse yaw, it is difficult to comment on how tip effects may impact the sign of the yawing moment coefficients relative to the rolling moment coefficients of the gapped wings.

The gapped wings have several limitations. Firstly, the gapped wings do not appear to be beneficial for rapid descent applications. While the gapped wings showed promise for roll control, the moment coefficients of the gapped wings were highly dependent on the coefficient of lift, which could require more complex controllers. Further, the gapped wings did not create as much rolling moment coefficient at lower coefficients of lift as conventional ailerons. Finally, the gaps may be mechanically complex to implement.

With these results on whiffing-inspired wings comes a call for further research in several disciplines. Whiffing is a unique and complex avian maneuver, and biological studies will provide ornithologists deeper insight into avian flight, and engineers further opportunities to leverage the behavior for bio-inspired work. Exploring the biological and aerodynamic mechanisms of avian whiffing would be valuable, including the influence of feather dynamics

on lift and drag. Since this work was focused on determining the aerodynamic characteristics of static gapped wings, developing an actuating prototype will be an important next step. The proposed sliding covers may be more mechanically complex to implement than an equivalent aileron. Therefore, prototyping would require studies into the most efficient actuation systems and manufacturing techniques for the sliding gap covers. Further, the sliding covers are not physically similar to the rotating feather mechanism, and thus research into a more feather-based actuation method may be required. In addition, the current results could be usefully extended by applying surface visualization techniques, and building CFD models. Surface visualization techniques and CFD models could resolve the aerodynamics of the gaps. In addition, CFD models could be used to thoroughly explore the gapped wing design space, enabling more rapid prototype iterations and optimization. CFD models and prototypes could also help evaluate the gapped wing control surface as a method of turbulence mitigation or gust alleviation [48–53].

5. Conclusion

Here we investigated if whiffing-inspired gapped wings could provide advantageous alternatives to spoilers for rapid descent or ailerons for banking. To do this, we tested wings with various numbers of gaps along the trailing edge at a low Re in a wind tunnel and extracted the lift, drag, rolling moment and yawing moment coefficients. Next, we calculated equivalent spoiler and aileron deflection angles based on previously published aerodynamic data, and compared the results to the gapped wings. Finally, we estimated the actuation force and work required to operate a hypothetical gapped wing prototype and compared to previously published actuation data on the representative spoiler and aileron. To the best of our knowledge, this is the first time that avian whiffing served as inspiration for a UAV control surface.

We found that, except for high angles of attack, increasing the number of gaps in the wing decreased the coefficient of lift, delayed stall, had negligible impact on the coefficient of drag, increased the rolling moment coefficient, and resulted in yaw in the same direction as roll both at low and very high angles of attack. The gapped wings did not decrease the coefficient of lift as much as a fully deflected spoiler, did not significantly increase the coefficient of drag, and required greater work to operate. Thus, they may not be a suitable alternative to spoilers for rapid descent.

The gapped wings did provide comparable aerodynamic performance to conventional ailerons: the nine-gap wing was able to produce an equivalent rolling moment coefficient to a representative aileron deflected 32.7° upwards at 13.5° angle of attack. Additionally, the nine-gap wing required 88.4% less force and 86.1% less work to achieve the same

rolling moment coefficient as the equivalent deflected aileron, making the gapped wings an attractive alternative to conventional ailerons for roll control of energy-constrained UAVs. Furthermore, these benefits occurred at a high coefficient of lift, suggesting that the gapped wing would be most suitable for a UAV flying at low airspeeds, and that it would be ideal to perform a pitch-up maneuver prior to banking to capture the maximum performance of the gapped wings. Their performance at high coefficients of lift also indicates that the gapped wings could extend the envelope over which UAVs perform roll maneuvers. In all, morphing trailing edge gaps inspired by whiffing could provide a novel control surface for roll control in energy-constrained UAVs.

Funding

This material is based upon work supported by the National Science Foundation under Grant No. EFRI C3 SoRo 1935216, the US Air Force Office of Scientific Research under Grants Numbered FA9550-16-1-0087, titled ‘Avian-Inspired Multifunctional Morphing Vehicles’ and FA9550-21-1-0325, titled ‘Towards Neural Control for Fly-by-Feel Morphing’ both monitored by Dr. B L Lee. PS is further supported by the National Science Foundation Graduate Research Fellowship Program under Grant No. DGE 1256260. Any opinions, findings, and conclusions or recommendations expressed in this material are those of the author(s) and do not necessarily reflect the views of the National Science Foundation.

Acknowledgments

Thank you to the AIMS lab for their support and guidance throughout this research, particularly Dr. Lawren Gamble and Dr. Christina Harvey for their technical expertise. Dr. Harvey provided initial drafts of MATLAB scripts used to automate wind tunnel testing. The authors would also like to thank the Duderstadt Fabrication Studio staff for manufacturing the wings. Finally, we would like to thank the technical staff in the Aerospace Engineering department for supporting this work technically and logistically, providing equipment, and manufacturing test apparatuses.

Data availability statement

The data that support the findings of this study are openly available at the following URL/DOI: doi.org/10.6084/m9.figshare.c.5735009 [54].

Appendix A. Uncertainty analysis

The standard combined uncertainty of the data (‘uncertainty’) was calculated according to the GUM [33]. We then determined and reported the expanded uncertainty of the data using a coverage factor of two, yielding an interval with a level of confidence of approximately 95%.

We included both type A and type B sources of variance in our uncertainty calculations, excluding the type B variance of the load cell. The type B variance of the load cell was specified by the manufacturer on the calibration certificate: the maximum measurement uncertainty was 1.00% of full-scale load at the 95% confidence level for all channels except moment about the z -axis, for which the maximum measurement uncertainty was 1.50%. The type B variance of the load cell represented one of the largest sources of relative uncertainty for the data. However, this uncertainty was mitigated by running multiple trials per wing and presenting the data in a cumulative averaged format. The type B variance of the load cell was therefore excluded from the plotted uncertainty.

The type A variation (standard error, or standard deviation of the mean) of the force, pressure, and temperature data were calculated using Zięba’s time series analysis method [55]. This method generally yielded more conservative (larger) uncertainty values due to autocorrelation of the data.

We accounted for correlations between the channels of the load cell in the error propagation, but correlations between the dynamic pressure and load cell readings were determined to be negligible and thus were excluded from calculations.

Appendix B. Determination of statistical significance

The results of this study are founded on relative data; that is, the differences between mean values of each gapped wing and the baseline wing mean values. In order to draw conclusions about these incremental data, we determined the statistical significance of each incremental data point. To do so, we calculated the expanded uncertainty of each difference of means, at an approximately 95% confidence level, following the methodology outlined in the GUM [33]. Note that this is similar to, but distinct from, a 95% confidence interval of the difference of means [33]. We first calculated the standard combined uncertainty of each gapped wing (mean) value and each baseline wing (mean) value. Then, we took the difference of the gapped wing mean and baseline wing mean, and calculated the corresponding standard combined uncertainty of that difference. Finally, we multiplied the standard combined uncertainty (of the difference of means) by a coverage factor (k) of two, per the GUM

[33]. This final product was the expanded uncertainty of the difference of means, at an approximately 95% confidence level. We set the null hypothesis to be zero. If the expanded uncertainty included the null hypothesis, we accepted the null, indicating that the difference in means was not statistically significant. In other words, there was no statistical evidence that the mean gapped wing value was different from the baseline wing value. If the expanded uncertainty did not encompass the null hypothesis, then we had evidence that the difference of means was statistically significant. That is, even accounting for the experimental uncertainty, there was statistical evidence that the gapped wing mean values were different from the baseline wing mean values. Determining the statistical significance of the incremental data provided a measure of certainty in our comparative results and conclusions. In summary, determining the statistical significance of the data provided a measure of reliability, and allowed us to compare the measurement results and accurately draw conclusions. In the results section, the statistically significant points are demarcated in the figures by a circled dot (⊙), and the insignificant points are marked with a dot (·).

ORCID iDs

Piper Sigrest  <https://orcid.org/0000-0003-1688-8676>

Daniel J Inman  <https://orcid.org/0000-0001-6195-1334>

References

- Böhmer C, Plateau O, Cornette R and Abourachid A 2019 Correlated evolution of neck length and leg length in birds *R. Soc. Open Sci.* **6** 181588
- Rysgaard G N 1942 When geese fly North *Bios* **13** 175–8
- Brotherston W 1964 The numbers and behaviour of geese in the Lothians and Berwickshire *Wildfowl* **15** 57–70
- Newton I, Thom V M and Brotherston W 1973 Behaviour and distribution of wild geese in south-east Scotland *Wildfowl* **24** 111–22
- Humphries D and Driver P 1970 Protean defence by prey animals *Oecologia* **5** 285–302
- Ogilvie M A and Wallace D I M 1975 Field identification of grey geese *Brit. Birds* **68** 57–67
- Gillmor R and Blurton Jones N G 1959 A goose-watching visit to northern Iceland *Wildfowl* **10** 114–7
- Sackl P 2000 Form and function of aerial courtship displays in black storks *Ciconia Nigra Acrocephalus* **21** 223–9
- Pete A E, Kress D, Dimitrov M A and Lentink D 2015 The role of passive avian head stabilization in flapping flight *J. R. Soc. Interface* **12** 20150508
- Levy Andrew 2009 The daily mail <https://dailymail.co.uk/news/article-1184566/Whiffle-wind-Pictures-flying-geeses-incredible-contortion-slow-down.html>
- Brown R H J 1963 The flight of birds *Biol. Rev.* **38** 460–89
- Hedrick T L, Usherwood J R and Biewener A A 2004 Wing inertia and whole-body acceleration: an analysis of instantaneous aerodynamic force production in cockatiels (*Nymphicus Hollandicus*) flying across a range of speeds *J. Exp. Biol.* **207** 1689–702
- Norberg U M 1974 Hovering flight in the pied flycatcher (*Ficedula Hypoleuca*) *Symp. Swimming and Flying in Nature* vol 2 (California Institute of Technology) pp 869–81
- Barlow J B, Rae W H Jr and Pope A 1999 *Low-Speed Wind Tunnel Testing* (New York: Wiley)
- Stephenson J D 1949 *The Effects of Aerodynamic Brakes Upon the Speed Characteristics of Airplanes* NACA, Ames Aeronautical Laboratory Publication NACA-TN-1939
- Müller W and Patone G 1998 Air transmissivity of feathers *J. Exp. Biol.* **201** 2591
- Marchman J F 1981 Aerodynamics of inverted leading-edge flaps on delta wings *J. Aircr.* **18** 1051–6
- Correia J, Roberts L S, Finnis M V and Knowles K 2014 Scale effects on a single-element inverted wing in ground effect *Aeronaut. J.* **118** 797–809
- Pankonien A M and Inman D J 2014 Aerodynamic performance of a spanwise morphing trailing edge concept *Presented at the Int. Conf. Adaptive Structures and Technologies* (The Hague, The Netherlands)
- Nedić J and Vassilicos J C 2015 Vortex shedding and aerodynamic performance of airfoil with multiscale trailing-edge modifications *AIAA J.* **53** 3240–50
- Davies H and Kirk F N 1942 A resume of aerodynamic data on air brakes *Publication Reports and Memoranda No. 2614* London National Aeronautical Establishment Library
- Purser E and Turner T R 1941 *Wind-Tunnel Investigation of Perforated Split Flaps for Use as Dive Brakes on a Rectangular NACA 23012 Airfoil* Washington NACA
- Laitone E V and Summers J L 1945 *An Additional Investigation of the High-Speed Lateral-Control Characteristics of Spoilers* Washington NACA Publication ACR 5D28
- Ni Z, Dhanak M and Su T-c 2019 Improved performance of a slotted blade using a novel slot design *J. Wind Eng. Ind. Aerodyn.* **189** 34–44
- Koss D, Steinbuch M and Shepshelovich M 1994 Design and experimental evaluation of a high-lift, mild-stall airfoil *12th Applied Aerodynamics Conf.* (Colorado Springs: American Institute of Aeronautics and Astronautics) pp 480–8
- Belamadi R, Djemili A, Ilinca A and Mdouki R 2016 Aerodynamic performance analysis of slotted airfoils for application to wind turbine blades *J. Wind Eng. Ind. Aerodyn.* **151** 79–99
- Weick F E and Shortall J A 1993 *The Effect of Multiple Fixed Slots and a Trailing-Edge Flap on the Lift and Drag of a Clark Y Airfoil* NACA, Langley Memorial Aeronautical Laboratory Publication NACA-TR-427
- Pankonien A M, Faria C T and Inman D J 2014 Synergistic smart morphing aileron: experimental quasi-static performance characterization *J. Intell. Mater. Syst. Struct.* **26** 1179–90
- Anderson J D Jr 2007 *Fundamentals of Aerodynamics* (New York: McGraw-Hill)
- Fischel J and Hagerman J R 1951 *Effect of Aspect Ratio and Sweepback on the Low-Speed Lateral Control Characteristics of Untapered Low-Aspect-Ratio Wings Equipped with Retractable Ailerons* NACA, Langley Memorial Aeronautical Laboratory Publication NACA-TN-2347
- Harvey C, Baliga V B, Goates C D, Hunsaker D F and Inman D J 2021 Gull-inspired joint-driven wing morphing allows adaptive longitudinal flight control *J. R. Soc. Interface* **18** 20210132
- Harvey C and Inman D J 2020 Aerodynamic efficiency of gliding birds vs comparable UAVs: a review *Bioinspiration Biomimetics* **16** 031001
- Joint Committee for Guides in Metrology 2008 *Evaluation of Measurement Data - Guide to the Expression of Uncertainty in Measurement* JCGM p 134 Publication JCGM100:2008
- Sadraey M H 2013 *Aircraft Design: A Systems Engineering Approach* (New York: Wiley)

- [35] Robinson A P, Tipping J, Cullen D M, Hamilton D, Brown R, Flynn A, Oldfield C, Page E, Price E, Smith A and Snee R 2016 Organ-specific SPECT activity calibration using 3D printed phantoms for molecular radiotherapy dosimetry *EJNMMI Phys.* **3** 12
- [36] Tasdemir M, Babat V and Yerlesen U 2014 Effect of friction and wear parameters on acrylonitrile butadiene styrene/aluminum-boron carbide-glass spheres polymer composites *Mechanika* **20** 407–13
- [37] Sun X-D 1993 Active control of aircraft using spoilers *Master's Dissertation* Imperial College of Science, Technology and Medicine, London
- [38] Chakraborty I, Jackson D, Trawick D R and Mavris D 2013 Development of a sizing and analysis tool for electrohydrostatic and electromechanical actuators for the more electric aircraft *Presented at the 2013 Aviation Technology, Integration, and Operations Conf.* (Los Angeles, CA, USA)
- [39] Scholz D Institution of Mechanical Engineers Aerospace Industries Division 1995 Development of a CAE-tool for the design of flight control and hydraulic systems *AeroTech 95* (Birmingham, UK October 1995) pp 1–21
- [40] Johnson H S and Hagerman J R 1950 *Wind-Tunnel Investigation at Low Speed of the Lateral Control Characteristics of an Unswept Untapered Semi-Span Wing of Aspect Ratio 3.13 Equipped with Various 25-Percent-Chord Plain Ailerons* (NACA, Langley Aeronautical Laboratory, Langley Memorial Aeronautical Laboratory) Publication NACA-TN-2199
- [41] Airfoil Tools 2022 Airfoil comparison airfoiltools.com (accessed 9 February 2022)
- [42] Carmichael B H 1981 *Low Reynolds Number Airfoil Survey vol I* (Capistrano Beach, CA: Low Energy Transportation Systems) Publication NASA-CR-165803-VOL-1
- [43] Thomas R, Bullock S, Bhandari U and Richardson T S 2015 Fixed-wing approach techniques for complex environments *Aeronaut. J.* **119** 999–1016
- [44] Carruthers A C, Thomas A L R, Walker S M and Taylor G K 2010 Mechanics and aerodynamics of perching manoeuvres in a large bird of prey *Aeronaut. J.* **114** 673–80
- [45] Di Luca M, Mintchev S, Heitz G, Noca F and Floreano D 2017 Bioinspired morphing wings for extended flight envelope and roll control of small drones *Interface Focus* **7** 20160092
- [46] John S, Rasheed A I and Reddy V K 2013 ASIC implementation of fuzzy-PID controller for aircraft roll control *Presented at the 2013 Int. Conf. Circuits, Controls and Communications* (CCUBE)
- [47] Deng Z, Wu L and You Y 2021 Modeling and design of an aircraft-mode controller for a fixed-wing VTOL UAV *Math. Probl. Eng.* **2021** 7902134
- [48] Mohamed A, Massey K, Watkins S and Clothier R 2014 The attitude control of fixed-wing MAVS in turbulent environments *Prog. Aerosp. Sci.* **66** 37–48
- [49] Panta A, Mohamed A, Marino M, Watkins S and Fisher A 2018 Unconventional control solutions for small fixed wing unmanned aircraft *Prog. Aerosp. Sci.* **102** 122–35
- [50] Mohamed A, Watkins S, Clothier R and Abdulrahim M 2014 Influence of turbulence on MAV roll perturbations *Int. J. Micro Air Veh.* **6** 175–90
- [51] Thompson M, Watkins S, White C and Holmes J 2011 Span-wise wind fluctuations in open terrain as applicable to small flying craft *Aeronaut. J.* **115** 693–701
- [52] Watkins S, Thompson M, Loxton B and Abdulrahim M 2010 On low altitude flight through the atmospheric boundary layer *Int. J. Micro Air Veh.* **2** 55–68
- [53] Mohamed A, Watkins S, Ol M V and Jones A R 2021 Flight-relevant gusts: computation-derived guidelines for micro air vehicle ground test unsteady aerodynamics *J. Aircr.* **58** 693–9
- [54] Sigrest P and Inman D J 2022 Data and codes supplement to: 'Avian whiffing-inspired gaps provide an alternative method for roll control' *Figshare*: <http://10.6084/m9.figshare.c.5735009>
- [55] Zięba A 2010 Effective number of observations and unbiased estimators of variance for autocorrelated data—an overview *Metrol. Meas. Syst.* **17** 3–16